Flexible Nanocrystalline-Titania/Polyimide Hybrids with High Refractive Index and Excellent Thermal Dimensional Stability

GUEY-SHENG LIOU,[1] PO-HAN LIN,[1] HUNG-JU YEN,[1] YANG-YEN YU,[2] WEN-CHANG CHEN[1,3]

[1]Institute of Polymer Science and Engineering, National Taiwan University, 1 Roosevelt Road, 4th Section, Taipei 10617, Taiwan

[2]Department of Materials Engineering, Mingchi University of Technology, 84 Gungjuan Road, Taishan, Taipei 243, Taiwan

[3]Department of Chemical Engineering, National Taiwan University, 1 Roosevelt Road, 4th Section, Taipei 10617, Taiwan

Received 20 November 2009; accepted 27 December 2009
DOI: 10.1002/pola.23914
Published online in Wiley InterScience (www.interscience.wiley.com).

ABSTRACT: In this study, a novel synthetic route was developed to prepare polyimide–nanocrystalline–titania hybrid optical films with a relatively high titania content (up to 50 wt %) and thickness (20–30 μm) from soluble polyimides containing hydroxyl groups. Two series of newly soluble polyimides were synthesized from the hydroxy-substituted diamines with various commercial tetracarboxylic dianhydrides. The hydroxyl groups on the backbone of the polyimides could provide the organic–inorganic bonding and resulted in homogeneous hybrid solutions by controlling the mole ratio of titanium butoxide/hydroxyl group. AFM, SEM, TEM, and XRD results indicated the formation of well-dispersed nanocrystalline-titania. The flexible hybrid films could be successfully obtained and revealed relatively good surface planarity, thermal dimensional stability, tunable refractive index, and high optical transparency. A three-layer antireflection coating based on the hybrid films was prepared and showed a reflectance of less than 0.5% in the visible range indicated its potential optical applications. © 2010 Wiley Periodicals, Inc. J Polym Sci Part A: Polym Chem 48: 1433–1440, 2010

KEYWORDS: functionalization of polymers; nanocomposites; polyimides; refractive index

INTRODUCTION Recently, with the rapid development of nanotechnology and nanoscience, research on polymer–inorganic hybrid materials have attracted considerable interest owing to the enhanced mechanical, thermal, magnetic, optical, electronic, and optoelectronic properties when compared to the corresponding individual polymer matrix or inorganic component.[1–3] *In situ* sol–gel hybridization approach made it possible to manipulate the organic/inorganic interfacial interactions at various molecular and nanometer length scales, resulting in homogeneous structures and thus overcoming the problem of nanoparticle agglomeration. For optical applications of these hybrid materials, such as high refractive index materials, optical waveguides, and antireflective films, the inorganic domains must be less than 40 nm to avoid scattering loss and retain the optical transparency.[4] Well-controlled morphology and phase separation are critical issues in the preparation of transparent hybrid films; thus sol–gel reaction was widely used for making transition metal oxide solids with fine-scaled microstructures. Therefore, particle sizes less than a couple of nanometers could easily be achieved in the derived gels, and the dimensions also could be maintained when subsequently crystallized at elevated temperatures.

Poly(methyl methacrylate) (PMMA),[5] polyimide (PI),[6,7] and others[8] have been extensively used for polymer–titania (TiO_2) hybrid materials as high refractive index materials. However, the relatively poor thermal stability of PMMA often limited their device applications, which might be overcome by using thermally stable PI as the organic matrix. Recently, Ueda laboratory have successfully prepared the PI–TiO_2 hybrid film containing 45 wt % silica-modified anatase-type TiO_2 nanoparticles with a refractive index of 1.81 at 632.8 nm.[9] Moreover, to control the titania domain size, the combination of *in situ* sol–gel processing with lower controlled molecular-weight polymer, coupling agent (such as 3-aminopropyl trimethoxysilane) or chelating agent (such as acetylacetone) was commonly used to prepare the hybrid materials.[6] However, using lower molecular weight polymers and additional coupling or chelating agents might suffer from poor storage stability, processability, and higher optical loss of the resulting hybrid materials. Furthermore, to obtain materials with high refractive index, a relatively large amount of TiO_2 nanocrystalline must be added. Thus, the flexible, transparent, and homogenous PI–TiO_2 hybrid thick film films with high titania content could not be achieved so far as we know.

In this contribution, a novel and simple synthetic route was developed to fabricate aromatic PI–nanocrystalline–titania hybrid thick films (up to 30 μm) with tunable titania contents, refractive index, and good optical transparency. The

Additional Supporting Information may be found in the online version of this article. Correspondence to: G.-S. Liou (E-mail: gsliou@ntu.edu.tw)
Journal of Polymer Science: Part A: Polymer Chemistry, Vol. 48, 1433–1440 (2010)

high molecular weight and organosoluble PIs with hydroxyl groups (**2,3-PHIc** and **2,7-PHIc**) were used to prepare their titania hybrid materials. These new naphthalene-based PIs revealed high refractive index values,[10] which were comparable with other heteroatom-containing polymers.[11] In addition, the lateral hydroxyl groups also provided the organic–inorganic bonding with titanium butoxide ($Ti(OBu)_4$). Therefore, no additional coupling agents or chelating ligands were used and highly homogeneous hybrid films with different titania contents could be successfully obtained. The morphologies of the prepared hybrid materials were characterized by AFM, SEM, TEM, and XRD. The thermal properties, optical transmittance, and refractive index dispersion of the prepared hybrid films were also investigated and described herein.

EXPERIMENTAL

Polymer Synthesis

Poly(o-hydroxy-imide)s PHIa-PHIe by One-Step Method

The synthesis of PI **2,3-PHIc** was used as an example to illustrate the general synthetic procedure. The stoichiometric mixture of the hydroxyl diamine **2,3-3** (0.51 g, 1.36 mmol), the dianhydride **4c** (0.42 g, 1.36 mmol), and a few drops of isoquinoline in *m*-cresol (10 mL) were stirred at ambient temperature under nitrogen. After the solution was stirred for 5 h, it was heated to reflux at 200 °C for 15 h. During this time, the water of imidization was allowed to distill from the reaction mixture along with *m*-cresol. The *m*-cresol was continually replaced so as to keep the total volume of the solution constant. After the solution was allowed to cool to ambient temperature, the viscous solution then was poured slowly into 300 mL of stirred methanol. The polymer that precipitated was collected by filtration, washed thoroughly with hot methanol, and dried under reduced pressure at 150 °C for 15 h. The inherent viscosity of the obtained PI **2,3-PHIc** was 0.79 dL/g (measured at a concentration of 0.5 g/dL in DMAc at 30 °C) The FTIR spectrum of **2,3-PHIc** (film) exhibited broad absorption bands in the region of 2500 to 3500 cm^{-1} (O—H stretch) and characteristic imide absorption bands at 1775 (asymetrical C=O), 1719 (symmetrical C=O), 1395 (C—N), and 743 cm^{-1} (imide ring deformation). Anal. Calcd for $(C_{38}H_{20}N_2O_9)_n$ $(648.57)_n$: C, 70.37%; H, 3.11%; N, 4.32%. Found: C, 68.54%; H, 3.59%; N, 4.74%

2,3-PI (without Hydroxyl Groups) by Two-Step Method via Chemical Imidization

The synthesis of PI **2,3-PI** was illustrated as follows: To a solution of 0.51 g (1.36 mmol) of diamine **2,3-3** in 9.5 mL of DMAc, 0.42 g (1.36 mmol) of **4c** was added in one portion. The mixture was stirred at room temperature overnight (*ca.* 12 h) to afford a viscous poly(amic acid) solution. The poly(amic acid) was subsequently converted to PI via a chemical imidization process by addition of pyridine 2 mL and acetic anhydride 5 mL, and the mixture was heated at 100 °C for 2 h to effect complete imidization. The resulting polymer solution was poured into 300 mL of methanol giving a fibrous precipitate, which was washed thoroughly with methanol, and collected by filtration. The precipitate was dissolved in 8 mL of DMAc, and the homogeneous solution was poured into a 9-cm glass culture dish, which was placed in a 90 °C oven for 12 h to remove the solvent. Then, the obtained film was further dried *in vacuo* at 180 °C for 6 h. The FTIR spectrum of **2,3-PI** film exhibited characteristic imide absorption bands at 1771 (asymetrical C=O), 1718 (symmetrical C=O), 1396 (C—N), and 747 cm^{-1} (imide ring deformation) without the absorption bands in the region of 2500 to 3500 cm^{-1} (O—H stretch).

Preparation of PI Films

A polymer solution was made by dissolving the PI sample in DMAc. The homogeneous solution was poured into glass Petri dish, then placed in an 80 °C oven overnight for the slow release of the solvent, and then the semidried film was further dried *in vacuo* at 180 °C for 8 h. The obtained films were 20–30-μm thick used for X-ray diffraction measurements, solubility tests, and thermal analyses.

Preparation of PI–Titania Hybrid Films

The synthesis of PI–titania hybrid **23TP50** was used as an example to illustrate the general synthetic route procedure. First, 0.12 g (0.18 mmole) of **2,3-PHIc** was dissolved in 6.0 mL of DMAc, and then 0.20 mL of HCl (37 wt %) was added very slowly into the PI solution and further stirred at room temperature for 30 min. Then, 0.50 mL (1.46 mmole) of $Ti(OBu)_4$ dissolved in 0.50 mL of butanol was added dropwise into the above solution by a syringe and then stirred at room temperature for 30 min. Finally, the resulting precursor solution of **2,3TP50** was filtered through a 0.45-μm PTFE filter and poured into a 6-cm glass Petri dish. The hybrid optical film could be obtained by subsequent heating program at 60 °C for 4 h, 150 °C for 3 h, and then 350 °C for 2 h under vacuum condition. After the curing process, hybrid films were immersed into water to peel off from the glass substrates and dried in vacuum. The obtained hybrid films were about 20–25 μm in thickness. For thin film preparation, the above precursor solution was diluted by DMAc and cast onto glass plate.

To study the effect of the hydroxyl groups on the morphology of the hybrid materials, a comparison film **2,3-PI30** without the hydroxyl group was also prepared using a similar procedure to that for **2,3TP30** except that **2,3-PI** was used to replace **2,3-PHIc**. In addition, the 100 wt % of titania film (**TP100**) was prepared according to the previously reported method.[7]

RESULTS AND DISCUSSION

Monomer Synthesis

The synthetic routes of bis(*o*-aminophenol) monomers are outlined in Supporting Information Scheme S1. The bis(*o*-aminophenol)s, 2,3-bis(4-amino-3-hydroxyphenoxy)naphthalene **(2,3-3)** and 2,7-bis(4-amino-3-hydroxyphenoxy)naphthalene **(2,7-3)**, were synthesized by the potassium carbonate-mediated nucleophilic substitution reaction of 2-benzyloxy-4-fluoronitrobenzene[12] **(1)** with 2,3-dihydroxynaphthalene and 2,7-dihydroxynaphthalene, followed by simultaneous

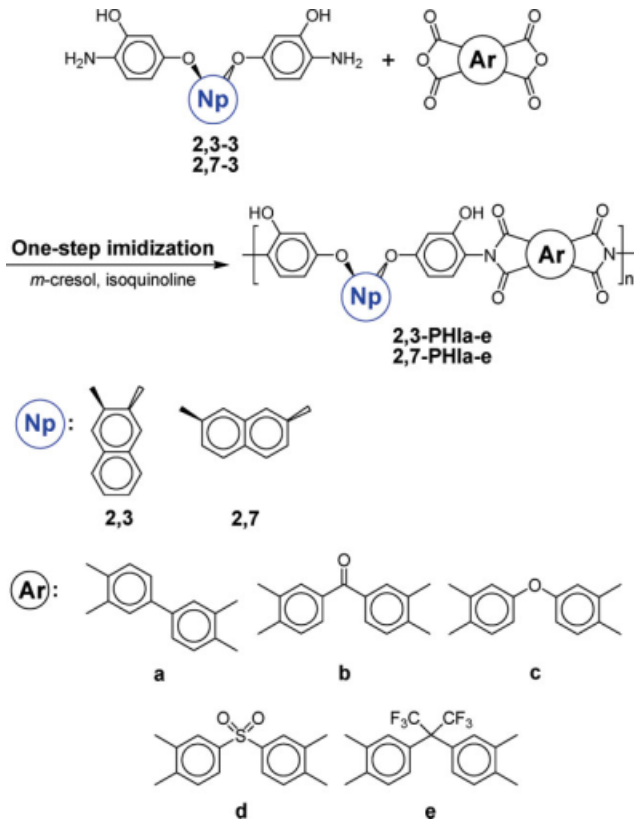

SCHEME 1 Polymer Synthesis. [Color figure can be viewed in the online issue, which is available at www.interscience.wiley.com.]

deprotection and reduction, respectively. Elemental analysis and FTIR spectroscopic techniques were used to identify the structures of the intermediate dinitro compounds and the hydroxyl diamine monomers, which were in good agreement with the previous literature.[13]

Polymer Synthesis

Two novel series of **2,3-PHI**s and **2,7-PHI**s were synthesized by the one-step method starting from hydroxyl-substituted diamine monomers, **2,3-3** and **2,7-3**, with aromatic tetracarboxylic dianhydrides in the presence of a catalytic amount of isoquinoline at 200 °C, respectively, (as shown in Scheme 1). On the other hand, the synthesis of **PHI**s by two-step method via chemical imidization was not suitable. Upon the chemical imidization process, the hydroxyl groups on the polymer backbone would react with acetic anhydride, thus **2,3-PI** was also prepared for comparison investigation. The formations of poly(*o*-hydroxy-imide)s were confirmed by elemental analysis, FTIR, and NMR spectroscopic techniques. The elemental analytic results of **2,3-PHI**s and **2,7-PHI**s are summarized in Supporting Information Table S1. FTIR spectra of **2,3-PHIc**, **2,7-PHIc**, and **2,3-PI** are shown in Supporting Information Figure S1. The **PHI**s exhibited broad absorption bands in the region of 2500 to 3500 cm^{-1} (O—H stretch) and characteristic imide absorption bands at 1775 (asymetrical C=O), 1719 (symmetrical C=O), 1396 (C—N), and 743 cm^{-1} (imide ring deformation). With the reaction of acetic anhydride and hydroxyl groups, **2,3-PI** also showed the characteristic imide bands but the absorption of hydroxyl groups disappeared. NMR spectra of **2,3-PHIc** are illustrated

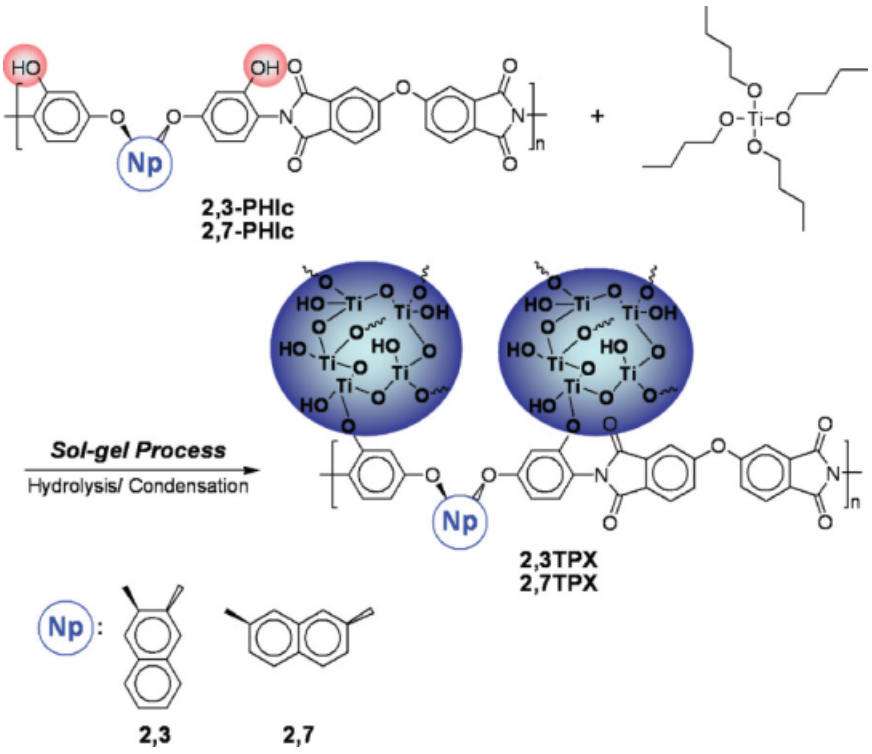

SCHEME 2 Hybrid Synthesis. [Color figure can be viewed in the online issue, which is available at www.interscience.wiley.com.]

TABLE 1 Reaction Composition and Properties of the **2,3-PHIc** Hybrid Films

	Reactant Compostition (wt %)		Hybrid Film TiO_2 Content (wt %)					
Sample	2,3-PHIc	$Ti(OBu)_4$	Theoretical	Experimental[a]	h (nm)[b]	R_q (nm)[c]	n[d]	v_D[e]
2,3-PHIc	100	0	0	0	498	2.029	1.67	17.8
2,3TP10	67.8	32.2	10	10.0	248	2.568	1.75	12.0
2,3TP30	35.4	64.6	30	29.6	393	2.335	1.81	12.0
2,3TP50	19.0	81.0	50	49.4	238	0.375	1.92	12.0
2,3TP70	9.1	90.9	70	69.9	131	0.208	1.96	14.2
TP100	0	100	100	100.0	132	–	1.99	17.0

[a] Experimental titania content estimated from TGA curves.
[b] h, Film thickness.
[c] R_q, The root mean square roughness.
[d] n, Refractive index at 633 nm.
[e] Abbe's number is given by $v_D = (n_{589} - 1)/(n_{486} - n_{656})$.

in Supporting Information Figure S2 and agree well with the proposed molecular structures. These obtained **PHI**s had inherent viscosities in the range of 0.35–0.90 dL/g, and the representative **2,3-PHIc**, **2,7-PHIc** had high weight-average molecular weights (M_w) of 51,900 and 48,200 Da, respectively, relative to polystyrene standards (Supporting Information Tables S1 and S2).

Polymer Properties

The solubility behavior of PIs was tested qualitatively and summarized in Supporting Information Table S3. All the PIs revealed high solubility in polar solvents such as *N*-methyl-2-pyrrolidinone (NMP), *N,N*-dimethylacetamide (DMAc), and *N,N*-dimethylformamide (DMF), and the enhanced solubility could be attributed to the introduction of flexible ether links, kinked bulky naphthalene moieties, and hydroxyl groups into the polymer main chain. Thus, the excellent solubility makes these polymers potential candidates for practical applications by spin- or dip-coating processes and further sol–gel process.

The thermal properties of the PIs were investigated by TGA and summarized in Supporting Information Table S4. All the aromatic PIs exhibited good thermal stability with insignificant weight loss up to 400 °C in nitrogen. Their 10% weight-loss temperatures in nitrogen and air were recorded at 460–515 °C and 465–515 °C, respectively. The carbonized residue (char yield) of these aromatic polymers was more than 53% at 800 °C in nitrogen atmosphere. The high char yields of these polymers could be ascribed to their high aromatic content.

The optical properties of the PIs were investigated by UV–vis and ellipsometer spectroscopy. The cutoff wavelengths (λ_o) from the UV–vis spectra are shown in Supporting Information Figure S3. The PIs **2,3-PHIc** and **2,3-PHIe** obtained from ether and hexafluoroisopropylidene linkages-containing dianhydrides exhibited higher transparent when compared with other ones. These results were attributed to the reduced intermolecular charge-transfer complex between alternating electron-donor (diamine) and electron-acceptor (dianhydride) moieties.

Refractive indices of the PIs could be calculated using the Lorentz–Lorenz equation:

$$\frac{n^2-1}{n^2+2} = \frac{4\pi}{3}\frac{\rho N_A}{M_w}\alpha = \frac{4\pi}{3}\frac{\alpha}{V_{mol}} \quad (1)$$

where n is the refractive index; ρ, the density; N_A, Avogadro's number; M_w, the molecular weight; α, the linear molecular polarizability; and V_{mol}, the molecular volume. As shown in eq 1, the molecular volume/density and polarizability were main factors of the refractive index. As the result, the lowest n values of **2,3-PHIe** and **2,7-PHIe** films (Supporting Information Figure S4) in the analogous series could be attributed to the lower electronic polarizability and a larger molecular volume of the hexafluoroisopropylidene groups. Considering the transparency and refractive index, **2,3-PHIc** and **2,7-PHIc** were used to prepare the titania optical hybrid materials for further investigations.

Synthesis of PI–Titania Hybrid Materials

The reaction route of PI and titania precursors is shown in Scheme 2, and the reaction compositions for **2,3TPX** and **2,7TPX** were summarized in Table 1 and Supporting Information Table S5, respectively. The flexible, transparent, and homogeneous PI–TiO_2 hybrid optical films with different titania contents have been successful prepared and the appearance is shown in Figure 1.

Properties of PI–Titania Hybrid Films

Structural Characterizations

The FTIR spectra of **2,3TP50** and **2,7TP50** films are shown in Supporting Information Figure S5; the absorption peak at 3000–3500 cm^{-1} of PI–TiO_2 thin film was attributed to the hydroxyl groups of the titania crystalline. In addition, the inorganic Ti—O—Ti band was also observed at 650–800 cm^{-1} and similar to that in the previous report.[7]

Thermal Properties

The thermal properties of the PI–TiO_2 hybrid materials were evaluated by TGA, DSC, TMA, and DMA, and summarized in Table 2. The TGA curves of the hybrid materials **2,3TPX** and **2,7TPX** are shown in Supporting Information Figures S6 and

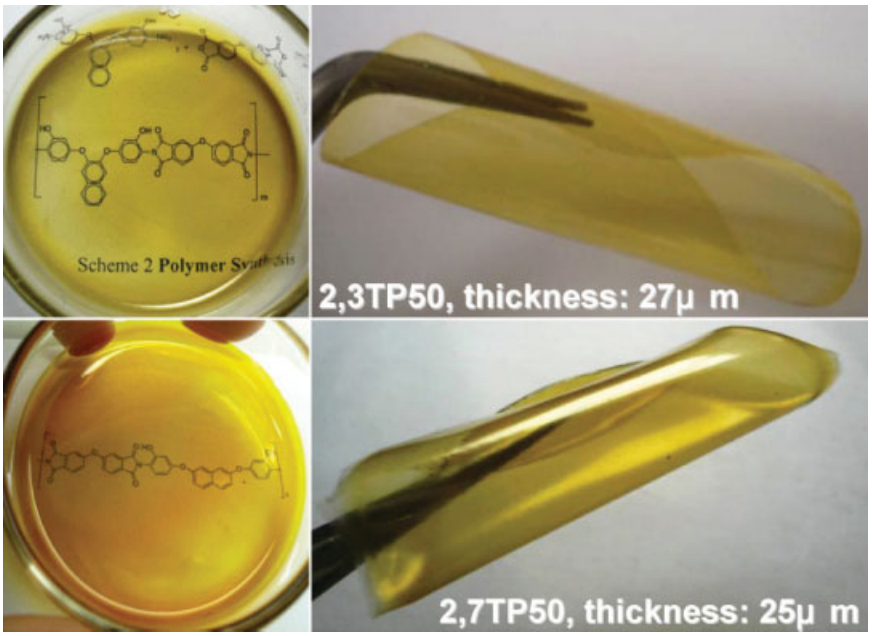

FIGURE 1 The photograph shows appearance of the high transparent, flexible PI–nanocrystalline–titania hybrid optical films.

S7, respectively, revealing high thermal stability of all hybrid materials. The titania contents in the hybrid materials could be estimated based on the char yields under air flow, which were in good agreement with the theoretical content and ensured the successfully incorporation of the nanocrystalline-titania. In addition, an initial 13.5% weight loss of PI **2,3-PHIc** observed between 380 and 490 °C showed the expulsion of two molecules of carbon dioxide per repeat unit. The proposed sequence is shown in Supporting Information Scheme S2, where the hydroxy-imide rearranged to a carboxybenzoxazole intermediate followed by decarboxylation above 350 °C to give the fully aromatic benzoxazole product.[14] On the other hand, the initial weight loss could not be found in the PI–titania hybrid materials, which provided another evidence of completely organic–inorganic bonding.

The DSC curves of the hybrid materials are shown in Supporting Information Figure S8. However, the unobvious T_g of these hybrid materials was because the nanocrystalline titania limited the mobility of the PI segment. Therefore, TMA of these materials was measured and the softening temperature increased from 273 to 386 °C with the increasing titania contents. The typical TMA thermogram of **2,3TP10** is illustrated in Supporting Information Figure S9. In addition, the dynamic mechanical thermal properties of the PI and hybrid thick films such as T_g, storage modulus E', and tan δ were also measured and shown in Figure 2. The T_g and storage modulus E' increased gradually with increasing titania content because the segmental chain mobility was restricted by crosslinking between PI chains and titania clusters. Moreover, **2,3TP50** still exhibited good damping behavior (tan $\delta > 0.3$) even with a high titania content.

The coefficiency of thermal expansion (CTE) is also one of important designing parameters for the application of polymer films in microelectronic field; therefore, CTE of the pure

TABLE 2 Thermal Properties of **2,3-PHIc** Hybrid Materials

	T_g(°C)[a]				T_d^5 (°C)[d]		T_d^{10} (°C)[d]		
Polymer	DSC	DMA	T_s (°C)[b]	CTE (ppm/K)[c]	N_2	Air	N_2	Air	R_{w800} (%)[e]
2,3-PHIc	271	273	273	81.3	435	430	460	465	53
2,3TP10	296	321	301	72.1	505	430	570	465	73
2,3TP30	340	333	313	59.1	515	430	590	465	78
2,3TP50	391	373	386	45.5	580	430	680	465	87

[a] Midpoint temperature of the baseline shift on the second DSC heating trace (rate: 20 °C/min) of the sample after quenching from 400 °C to 50 °C (rate: 200 °C/min) in nitrogen. Dynamic mechanical thermal analysis (DMA) was performed on PI film specimens (15-mm long, 8-mm wide, and 40–50-μm thick) at a heating rate of 3 °C/min with a load frequency of 1 Hz in air.
[b] Softening temperature measured by TMA with a constant applied load of 10 mN at a heating rate of 10 °C/min by penetration mode.
[c] The CTE data were determined over a 50–200 °C range by expansion mode.
[d] Temperature at which 5% and 10% weight loss occurred, respectively, recorded by TGA at a heating rate of 20 °C/min and a gas flow rate of 30 cm^3/min.
[e] Residual weight percentage at 800 °C in nitrogen.

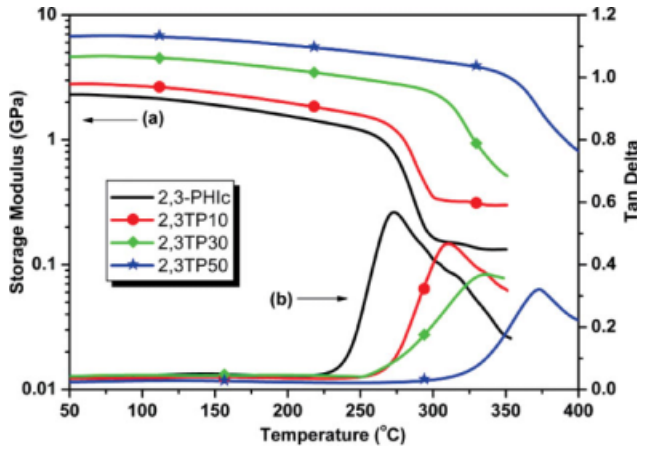

FIGURE 2 (a) Storage modulus and (b) Tan delta curves of **2,3-PHIc** hybrid materials. [Color figure can be viewed in the online issue, which is available at www.interscience.wiley.com.]

PI film and PI–TiO_2 hybrid films was measured and summarized in Table 2. Inorganic reinforced components often revealed much lower CTE values than that of organic matrix, which suppressed CTE of the resulting hybrid materials. Thus, CTE of the organic–inorganic hybrids decreased with increasing of volume fractions of inorganic reinforcement.

Morphology Analyses

The SEM images of **2,3-PHIc** and **2,7-PHIc** hybrid films are shown in Supporting Information Figures S10 and S11, respectively, which exhibited uniform surface without any apparent microstructural separation or significant titania aggregates. In addition, the SEM image of **2,3-PI30** in Supporting Information Figure S10(d) shows severe phase separation with a large aggregated domain. These results demonstrate that the hydroxyl groups on PI played important roles for not only enhancing the solubility and providing bonding sites with TiO_2 but also effectively improving the resultant dispersity and morphology stability of these hybrid materials. The AFM images of the **2,3-PHIc** and **2,7-PHIc** hybrid thin films are shown in Supporting Information Figure S12 and S13, and the analyzed root mean square surface roughness (R_q) for the hybrid films is listed in Table 1 and Supporting Information Table S5, respectively. The ratio of surface roughness to film thickness (R_q/h) was less than 0.15%, implying the excellent surface planarity of the hybrid films could be obtained. Furthermore, the TEM image of the **2,3TP50** film shown in Figure 3(a) exhibited the titania nanocrystallites with the average size of 3–5 nm well dispersed in the hybrid material. The XRD patterns of the hybrid films shown in Figure 3(b) revealed that the matrix PI was amorphous, and the intensity of a titanina crystalline peak gradually increased in the range $2\theta = 23°–27°$ with increasing titania content suggesting that the titania clusters were well dispersed in PIs because of hydrolysis-condensation reactions occurred between $Ti(OBu)_4$ and pendant hydroxyl groups of PI. The clear titania crystallization could be observed in **2,3TP70**, four peaks, 25.5°, 38.4°, 48.3°, and 54.8°, corresponding to the (101), (112), (200), and (211) crystalline planes of the anatase titania phase, respectively.[15,16] The broad width of the peaks was because the scattering of X-ray resulted from the small size of the titania nanocrystalline grain, which was also well agreed with the results from TEM images. The average crystallite sizes could be estimated to be ~5 nm for **2,3TP50** by using the Debye-Scherrer equation:

$$B = \frac{0.94 \times \lambda}{d \times \cos\theta} \tag{2}$$

Note that B is the peak's full width at half maximum (FWHM), θ is the peak position, and d is the average diameter of the crystallite in nanometer.

Optical Properties

UV–vis spectra of the hybrid thin films and thick films are shown in Figure 4. The cutoff wavelengths of the hybrid films in the UV region were contributed from the chromophores of PI, and all the thick hybrid films exhibited much higher optical transparency than Kapton [Fig. 4(b)]. In addition, the absorption intensity of the cutoff wavelengths was enhanced and the corresponding band edge was red-shifted (Supporting Information Table S6) with increasing the titania content. Such band shift could usually be observed for titania sizes less than 10 nm,[7] indicating that highly homogeneous PI–nanocrystalline–titania hybrid materials were obtained.

The refractive index dispersion results are shown in Figure 5 and Supporting Information S14, and the variation in

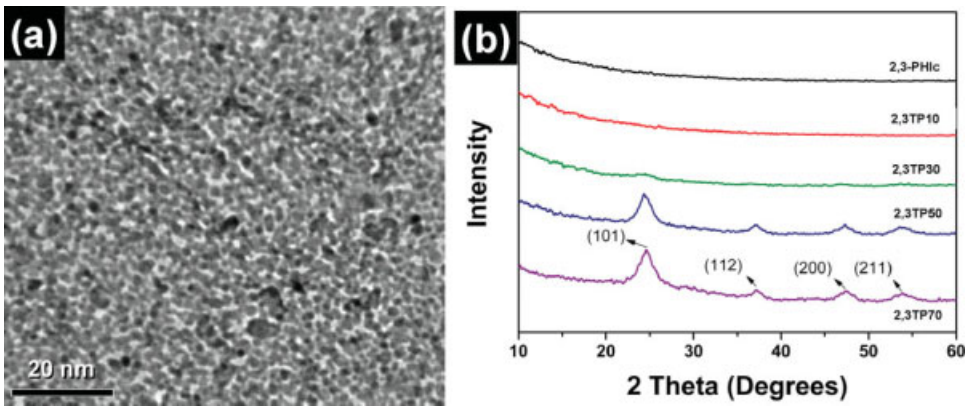

FIGURE 3 (a) TEM images of the **2,3TP50** hybrid film and (b) XRD patterns of the **2,3-PHIc** hybrid materials. [Color figure can be viewed in the online issue, which is available at www.interscience.wiley.com.]

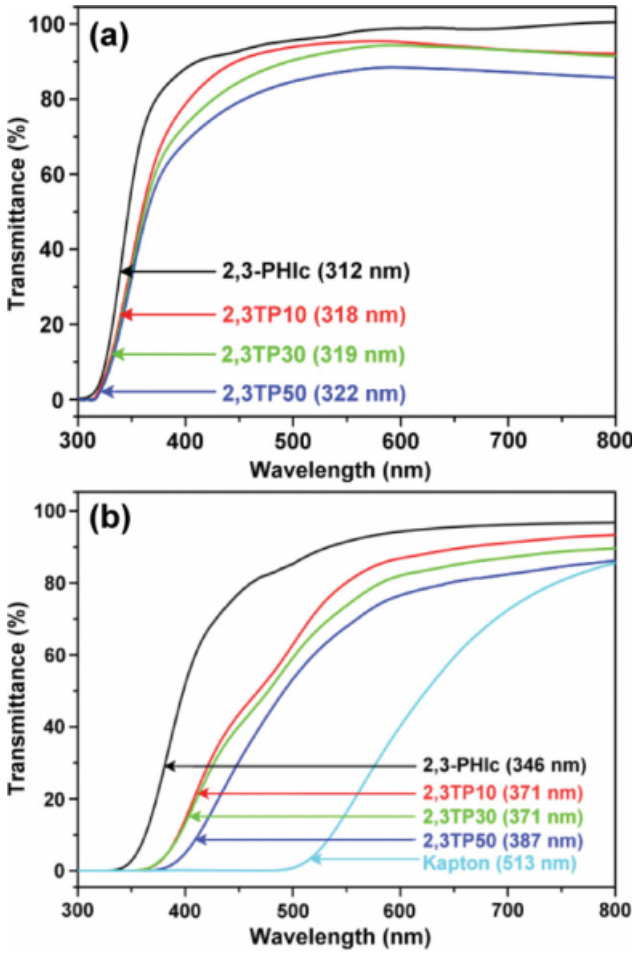

FIGURE 4 Transmittance UV–visible spectra of **2,3-PHIc** hybrid materials: (a) thin films (thickness: 100–500 nm) and (b) thick films (thickness: 20–30 μm). [Color figure can be viewed in the online issue, which is available at www.interscience.wiley.com.]

refractive index at 633 nm with titania content was depicted in insert figures. The refractive index increased linearly with titania contents suggesting that the Ti—OH groups of the hydrolyzed precursors condensed progressively to form the Ti—O—Ti structures and resulted in an enhanced refractive index. It also indicated that using a soluble PI with hydroxyl groups on each repeating units is a successful approach for preparing titania hybrid materials. Besides, the evaluated color coordinates of the hybrid films summarized in Supporting Information Table S6 also suggested excellent optical transparency in the visible region. Combining the issues of thickness, flexibility, and optical transparency, the PI–titania hybrid optical thick film **2,3TP50** (20–30 μm in thickness) in this article demonstrated the highest refractive index (1.92) to the best of our knowledge comparing with other polymer–titania hybrid materials.[5–8]

Multilayer Antireflection Coatings

The structure of three-layer antireflective coating on the glass substrate and the reflectance spectra are shown in Figure 6. The glass substrate revealed a refractive index (n = 1.52) higher than air (n = 1.0) and leaded an average reflectance of 4.4% in the visible range. The reflectance could be reduced significantly via the three-layer antireflection coating consisted of **Colloid SiO_2**, **2,3TP50**, and **2,3TP10** for the first, second, and third layer, respectively. To reduce reflection through adjusting phase of light, the optical thickness (physical thickness × refractive index) was designed to be 0.25 λ_o, 0.5 λ_o, and 0.25 λ_o (λ_o = 550 nm) for the three-layer structure. Thus, the prepared film thickness and refractive index of **Colloid SiO_2**, **2,3TP50**, and **2,3TP10** were 96 nm and 1.29; 140 nm and 1.96; 80 nm and 1.77, respectively. As shown in Figure 6, the reflectance of prepared antireflection

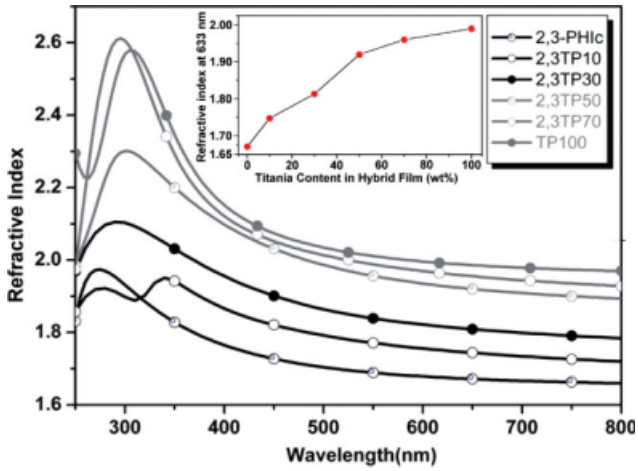

FIGURE 5 Variation of the refractive index of the **2,3-PHIc** hybrid materials with wavelength. The insert figure shows the variation of refractive index at 633 nm with titania content. [Color figure can be viewed in the online issue, which is available at www.interscience.wiley.com.]

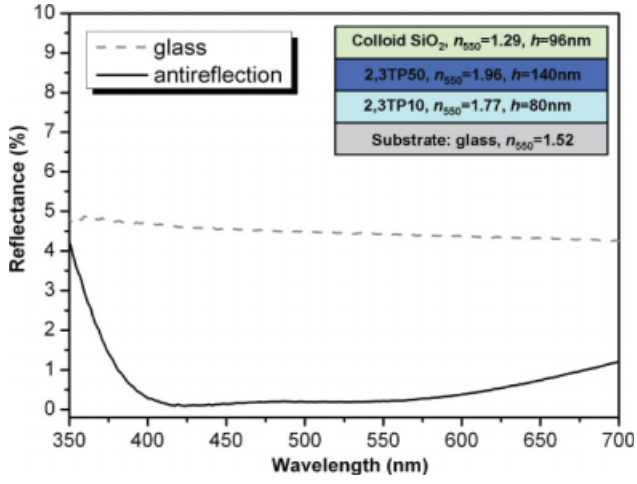

FIGURE 6 Variation of the reflectance with wavelength: optical glass and the three-layer antireflection coating. The insert figure shows the structure of the three-layer antireflection coating. [Color figure can be viewed in the online issue, which is available at www.interscience.wiley.com.]

coatings was less than 0.5% in the visible range (400 nm to 700 nm), which was significantly smaller than that of the glass with 4.4%. It suggested the potential application of the prepared PI–titania hybrid films in optical devices.

CONCLUSIONS

Two series of novel soluble PIs were synthesized from the hydroxy-substituted diamines with various commercial tetracarboxylic dianhydrides, respectively. Furthermore, high transparency and tunable refractive index PI–titania hybrid optical films were successfully synthesized from soluble hydroxyl-substituted PIs with titanium butoxide by controlling the organic/inorganic mole ratio. The refractive index of hybrid thin films revealed good surface planarity, high thermal stability, tunable refractive index, and high optical transparency in the visible range. Three-layer antireflective coating based on the hybrid films possessed reflectance of less than 0.5% in the visible range, suggesting potential optical applications of the novel PI–titania hybrid optical films. Furthermore, the thick titania hybrid films could also be achieved even with the relatively high titania content (50 wt %) and refractive index (1.92). To the best of our knowledge, the refractive index and titania content were the highest among the polymer–titania hybrid optical thick films (20–30 μm in thickness).

The authors are grateful to the National Science Council of the Republic of China for financial support of this work.

REFERENCES AND NOTES

1 (a) Beecroft, L. L.; Ober, C. K. Chem Mater 1997, 9, 1302–1317; (b) Sanchez, C.; Lebeau, B.; Chaput, F.; Boilot, J. P. Adv Mater 2003, 15, 1969–1994; (c) Laine, R. M. J Mater Chem 2005, 15, 3725–3744; (d) Zelcer, A.; Donnio, B.; Bourgogne, C.; Cukiernik, F. D.; Guillon, D. Chem Mater 2007, 19, 1992–2006; (e) Zhou, Z.; Franz, A. W.; Hartmann, M.; Seifert, A.; Muller, T. J. J.; Thiel, W. R. Chem Mater 2008, 20, 4986–4991; (f) Pereira, F.; Valle, K.; Belleville, P.; Morin, A.; Lambert, S.; Sanchez, C. Chem Mater 2008, 20, 1710–1718; (g) Lin, Y. Y.; Chen, C. W.; Chu, T. H.; Su, W. F.; Lin, C. C.; Ku, C. H.; Wu, J. J.; Chen, C. H. J Mater Chem 2007, 17, 4571–4576.

2 (a) Functional Hybrid Materials; Gomez-Romero, P.; Sanchez, C., Eds.; Wiley-VCH: Weinheim, 2004; (b) Kickelbick, G. Hybrid Materials: Synthesis, Characterization, and Applications; Wiley-VCH: Weinheim, 2007.

3 (a) Li, T. L.; Hsu, S. L. C. J Polym Sci Part A: Polym Chem 2009, 47, 1575–1583; (b) Ye, Y. S.; Yen, Y. C.; Chen, W. Y.; Cheng, C. C.; Chang, F. C. J Polym Sci Part A: Polym Chem 2008, 46, 6296–6304; (c) Wahab, M. A.; Mya, K. Y.; He, C. J Polym Sci Part A: Polym Chem 2008, 46, 5887–5896; (d) Liu, Y. L.; Tseng, M. C.; Fangchiang, M. H. J Polym Sci Part A: Polym Chem 2008, 46, 5157–5166; (e) Yuen, S. M.; Ma, C. C. M.; Chiang, C. L.; Teng, C. C.; Yu, Y. H. J Polym Sci Part A: Polym Chem 2008, 46, 803–816.

4 Althues, H.; Henle, J.; Kaskel, S. Chem Soc Rev 2007, 36, 1454–1465.

5 (a) Chen, W. C.; Lee, S. J.; Lee, L. H.; Lin, J. L. J Mater Chem 1999, 9, 2999–3003; (b) Lee, L. H.; Chen, W. C. Chem Mater 2001, 13, 1137–1142; (c) Yuwono, A. H.; Zhang, Y.; Wang, J.; Zhang, X. H.; Fan, H.; Ji, W. Chem Mater 2006, 18, 5876–5889.

6 (a) Nandi, M.; Conklin, J. A.; Salvati, L.; Sen, A. Chem Mater 1991, 3, 201–206; (b) Chang, C. C.; Chen, W. C. J Polym Sci Part A: Polym Chem 2001, 39, 3419–3427; (c) Guevel, X. L.; Palazzesi, C.; Prosposito, P.; Giustina, G. D.; Brusatin, G. J Mater Chem 2008, 18, 3556–3562.

7 Su, H. W.; Chen, W. C. J Mater Chem 2008, 18, 1139–1145.

8 (a) Wang, B.; Wilkes, G. L.; Hedrick, J. C.; Liptak, S. C.; McGrath, J. E. Macromolecules 1991, 24, 3449–3450; (b) Chen, W. C.; Lee, L. H.; Chen, B. F.; Yen, C. T. J Mater Chem 2002, 12, 3644–3648; (c) Lu, S. R.; Zhang, H. L.; Zhao, C. X.; Wang, X. Y. Polymer 2005, 46, 10484–10492; (d) Liu, J. G.; Ueda, M. J Mater Chem 2009, 19, 8907–8919; (e) Vestberg, R.; Piekarski, A. M.; Pressly, E. D.; Berkel, K. Y. V.; Malkoch, M.; Gerbac, J.; Ueno, N.; Hawker, C. J. J Polym Sci Part A: Polym Chem 2009, 47, 1237–1258.

9 Liu, J. G.; Nakamura, Y.; Ogura, T.; Shibasaki, Y.; Ando, S.; Ueda, M. Chem Mater 2008, 20, 273–281.

10 Kawasaki, S.; Yamada, M.; Kobori, K.; Jin, F.; Kondo, Y.; Hayashi, H.; Suzuki, Y.; Takata, T. Macromolecules 2007, 40, 5284–5289.

11 (a) Liu, J. G.; Nakamura, Y.; Shibasaki, Y.; Ando, S.; Ueda, M. Macromolecules 2007, 40, 4614–4620; (b) Liu, J. G.; Nakamura, Y.; Suzuki, Y.; Shibasaki, Y.; Ando, S.; Ueda, M. Macromolecules 2007, 40, 7902–7909; (c) You, N. H.; Suzuki, Y.; Yorifuji, D.; Ando, S.; Ueda, M. Macromolecules 2008, 41, 6361–6366.

12 Imai, Y.; Park, K. H.; Kakimoto, M. A. J Polym Sci Part A: Polym Chem 1998, 36, 1987–1994.

13 Chern, Y. T. U.S. Patent 20,060,241,187, 2006.

14 Likhatchev, D.; Gutierrez-Wing, C.; Kardash, I.; Vera-Graziano, R. J Appl Polym Sci 1996, 59, 725–735.

15 (a) Yuwono, A. H.; Xue, J.; Wang, J.; Elim, H. I.; Ji, W.; Li, Y.; White, T. J. J Mater Chem 2003, 13, 1475–1479; (b) Yuwono, A. H.; Liu, B.; Xue, J.; Wang, J.; Elim, H. I.; Ji, W.; Li, Y.; White, T. J. J Mater Chem 2004, 14, 2978–2987.

16 (a) Eder, D.; Windle, A. H. J Mater Chem 2008, 18, 2036–2043; (b) Miyauchi, M. J Mater Chem 2008, 18, 1858–1864; (c) Yu, A.; Lu, G. Q.; Drennan, J.; Gentle, I. R. Adv Funct Mater 2007, 17, 2600–2605; (d) Fattakhova-Rohlfing, D.; Wark, M.; Brezesinski, T.; Smarsly, B. M.; Rathousky, J. Adv Funct Mater 2007, 17, 123–132.